CrossMark

MOLECULAR TOXICOLOGY

Experimental and computational insights on the recognition mechanism between the estrogen receptor α with bisphenol compounds

Huiming Cao[1,2,3] · Fengbang Wang[1,2] · Yong Liang[3] · Hailin Wang[1] · Aiqian Zhang[1,2] · Maoyong Song[1,2]

Abstract Certain bisphenols (BPs) have been regarded as endocrine-disrupting chemicals due to their structural similarities to bisphenol A (BPA), a well-known weak estrogenic chemical. However, very limited data are currently available on the relationship between estrogenic activity and the structure of BP analogs. Therefore, we systematically investigated the estrogenic potency of 14 selected BP analogs with typical structures using experimental and computational methods. Most of the tested BP analogs exhibited weak estrogenic activities in both cell proliferation and MVLN assays with the exception of TBBPA, TCBPA and TBBPS. Molecular modeling techniques have been performed to investigate the dynamic structural characteristics of recognition processes between BPs and estrogen receptor α (ERα) at the atomic level. Thr347 was identified as the key residue responsible for the recognition of TBBPA, TCBPA and TBBPS by means of induced-fit H-bonding interactions in the binding pocket of ERα, whereas other BPs, in turn, rely on the alternative formation of H-bonds with His524. Subsequent allosteric modulation interferes significantly with the stability of helix 12 that is crucial for the transcriptional activity of ERα. These structural perturbations that are induced by the three compounds were further confirmed to reduce the recruitment potency of co-activators more than other BPs based on calculations of binding free energies, which is in line with observed experimental transcriptional activities. Our findings may help to elucidate the estrogenic potency of BPs with different molecular structures.

Keywords Estrogen receptor α · Bisphenols · Estrogenic activity · Molecular dynamics simulations

✉ Aiqian Zhang
    aqzhang@rcees.ac.cn

✉ Maoyong Song
    mysong@rcees.ac.cn

1   State Key Laboratory of Environmental Chemistry and Ecotoxicology, Research Center for Eco-Environmental Sciences, Chinese Academy of Science, Beijing 100085, People's Republic of China

2   University of Chinese Academy of Sciences, Beijing 100049, People's Republic of China

3   Institute of Environment and Health, Jianghan University, Wuhan 430056, People's Republic of China

Introduction

Endocrine disrupting chemicals (EDCs) have raised extensive concerns in recent years. Bisphenol A (BPA), a representative EDC, has been detected in various environmental locations (Vandenberg et al. 2007). This compound can mimic natural hormones and can bind competitively to a number of nuclear receptors such as androgen receptors (ARs) (Molina-Molina et al. 2013), estrogen receptors (ERs) (Molina-Molina et al. 2013) and peroxisome proliferator-activated receptors (PPARs) (Riu et al. 2011). In particular, BPA acts as a weak ER binder and disorders the biological functions of the endogenous ligand 17β-estradiol (E2), which causes adverse effects on the reproductive system and embryonic development in vivo (Henley and Korach 2006; Vom Saal et al. 2007). Therefore, replacing BPA with alternative chemicals in industrial applications was proposed to lessen the deleterious effects on public health (Chen et al. 2002; Rosenmai et al. 2014).

The substitute bisphenol congeners are structurally similar to BPA and contain two phenol rings with a bridging carbon or other structural groups. Due to the increased production and consumption of these compounds, there is also concern regarding their public and environmental health effects (Ng et al. 2015; Rosenmai et al. 2014; Yang et al. 2011). The estrogen receptors ERα and ERβ, the main receptor targets of BPA, were studied for their interactions with the alternative compounds (Kitamura et al. 2005). The endocrine disrupting activities of these substitutes also were widely reported (Molina-Molina et al. 2013; Teng et al. 2013). For instance, bisphenol AF (BPAF) and bisphenol C (BPC) influenced the transcriptional activity of the ERs both in vitro and in vivo (Delfosse et al. 2012; Li et al. 2012, 2013; Molina-Molina et al. 2013).

Generally, an ERα agonist triggers gene transcription through a conformational change from an apo state to an active state when binding to the C-terminal ligand-binding domain (LBD) of ERα (Brzozowski et al. 1997; Shiau et al. 1998). The ER ligand-binding domain (LBD) is composed of twelve alpha helices and a beta sheet. When E2 enters into the mostly hydrophobic pocket which is located in the central domain of the ERα LBD, its allosteric modulation induces a conformational change in alpha helix 12 (H12), thereby generating a surface site for the subsequent recruitment of co-activator with conserved LxxLL structures (Chang et al. 1999; Heery et al. 1997). In contrast, an antagonist induces a structural reconstruction of LBD by transforming H12 into a co-activator binding site and then impeding recruitment of the co-activator. Such structural repositioning of H12 usually requires the steric obstruction of antagonists. Classical antagonists, such as ICI164,384 (Pike et al. 2001) and 4-hydroxytamoxifen (OHT) (Shiau et al. 1998), possess bulky groups that interact with H12 and move it away from the agonist conformation. Previous reports (Delfosse et al. 2012, 2014) showed that the crystal structures of ERα in complex with BPA, BPAF and BPC have quite different binding poses in the ligand-binding pocket of ERα. For example, BPA acted as the natural agonist E2 (Brzozowski et al. 1997) and induced the agonist-bound conformation in which H12 covers the LBD pocket, whereas BPC triggered the repositioning of H12 into the ERα surface groove and adopted a similar LBD conformation that was induced by the typical antagonist OHT (Shiau et al. 1998). In particular, BPAF exhibited two distinct poses (BPA-like and BPC-like ones) in each monomer in the crystalized ERα homodimer, whereas only unique pose has been obtained for co-crystalized endogenous hormone E2, weak agonist BPA or weak antagonist BPC in their ERα complexes under the same crystal condition (Delfosse et al. 2012). It implied that BPAF presents two different stable binding modes with different recognition characteristics in the E2-bound pocket of ERα, associating with diverse allosteric modulations and the resulting transcriptional activities. Therefore, the bisphenol compounds were speculated to act as agonists, partial agonists or antagonists when binding to ERα. However, detailed information concerning the underlying molecular mechanisms of other bisphenol compounds that involve the transcriptional activity of ERs is still limited.

In this study, we first investigated the estrogenic and anti-estrogenic activities of 14 BPs (Fig. 1) using reporter gene and cell proliferation assays. Subsequently, based on the wild type ERα structure, each BP was docked into the E2 binding pocket to explore their binding modes and to predict their binding affinities for ERα. Furthermore, a molecular dynamics (MD) simulation (Liu et al. 2015; Singh et al. 2015) was applied to obtain insight into the dynamic binding process of the ligands and the ligand-induced conformational changes at an atomic level. Ultimately, triple complex structures for the ligand-ERα-cofactor were constructed to probe the impact of the BPs on the binding of co-activator to ERα. Our experimental findings together with computational simulations may provide insights into the relationship between the estrogenic potency of BPs and their different molecular structures.

Materials and methods

Regents

BPA, BPB, BPE, BPF, BPS, BPAF, BPAP, Nonox DCP (NDCP), 2,4-dihydroxybenzophenone (DHBP), dihydroxydiphenyl sulfide (TDP), tetramethylbisphenol A (TMBPA), tetrabromobisphenol A (TBBPA) and tetrachlorobisphenol A (TCBPA) were obtained from TCI (Tokyo, Japan), and all compounds had a purity of 98% or greater unless otherwise stated. 17β-estradiol (E2; 99% pure) was obtained from Alfa Aesar (Ward Hill, MA, USA). A high affinity estrogen receptor antagonist, fulvestrant (ICI 182,780; 98% pure), was purchased from Sigma-Aldrich (St. Louis, MO, USA). BPs, E2 and ICI 182,780 were dissolved in methanol to form stock solutions and were stored in the dark. Ultrapure water (18.3 MU) was produced using a Milli-Q system (Millipore, Billerica, MA, USA). All other compounds used in this study were of analytical grade.

E-screen assay

The E-screen assay used in this study was conducted as previously described (Molina-Molina et al. 2013). Briefly, human MCF-7BUS breast adenocarcinoma cells were cultured in 100 mm culture dishes in a humidified atmosphere of 5% CO_2 at 37 °C. Prior to the E-Screen assay, cells were harvested and then plated into the interior 60 wells

Fig. 1 Chemical structure of 14 bisphenols in this study
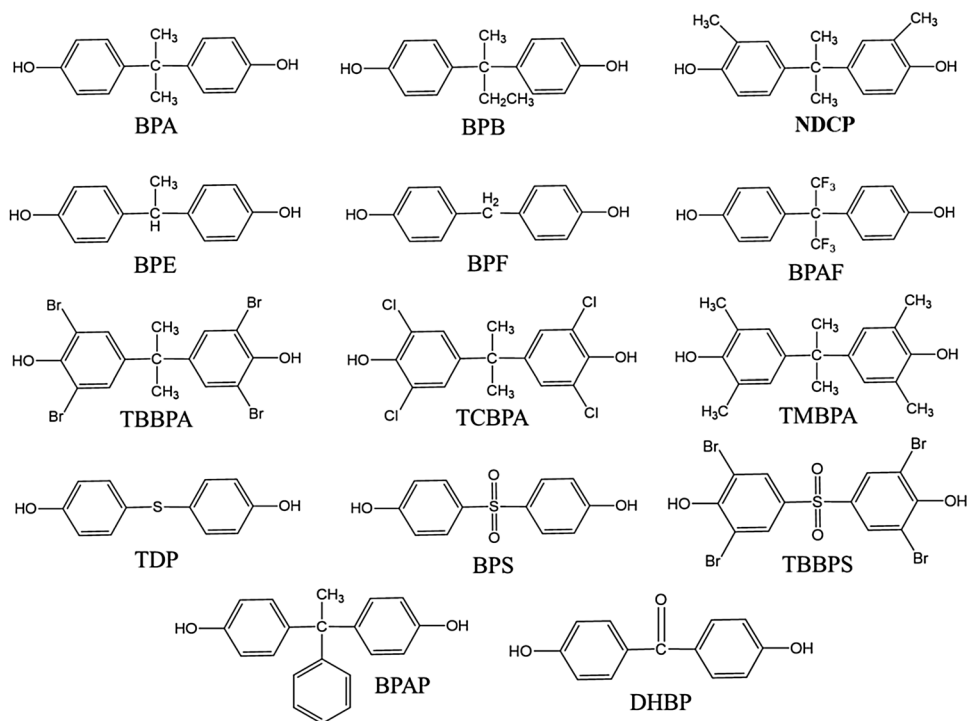
of 96-well plates at a density of 4000 cells per well. The cells were starved in steroid-free (SF) medium for 48 h to minimize the basal hormonal activity during the assays. SF medium consisted of phenol red-free Dulbecco's modified Eagle's medium with 5% charcoal dextran stripped fetal bovine serum, 100 U/mL streptomycin-penicillin and 2 mM glutamine. The tested chemicals were diluted with SF medium, and serial dilutions were prepared (from 5×10^{-8} to 5×10^{-5} M) and added to the cells. A concentration range of 5×10^{-13} to 5×10^{-9} M E2 was used as the positive control. Experimental medium was added to one column of each plate as a negative control. The medium was replaced with fresh culture medium containing the test material every 3 days. In response to the ERα agonists, the mitotic effect leads to the proliferation of MCF-7 cells. A WST-1 proliferation kit (Roche Diagnostics, Mannheim, Germany) was used to assess proliferation after 6 days of exposure according to the kit instructions. The absorbance of the WST-1 solution was measured using a microplate reader (Varioskan Flash, Thermo Fisher Scientific, Waltham, MA, USA) at 450 nm. The cell proliferation effects were expressed as a percentage of the maximal absorbance of the positive control. All assays were performed on separate plates in triplicate.

MVLN assay

The relative estrogenic activities of the tested compound were determined using an MVLN assay. The MVLN cell line was kindly provided by J.P. Giesy (Michigan State University, East Lansing, MI, USA). This cell line was stably transfected with the luciferase reporter gene and an estrogen-responsive element, and ER agonists can induce the production of luciferase. A concentration range of 1×10^{-14} to 1×10^{-9} M E2 was used as a positive control. The concentrations of test BPs were the same as the E-screen assay. The estrogenic activity of each compound was determined as previously described (Song et al. 2006, 2014). Briefly, cells were seeded into the 60 interior wells of a 96-well culture plate at a density of 5×10^4 cells per well. Cells were cultured under aseptic conditions in a humidified CO_2 incubator at 37 °C with 5% CO_2. Prior to the exposure, the cells were starved in SF medium for 48 h. Luciferase activity was measured using the LucLite kit according to the manufacturer's protocol. Luminescence was measured using a Microplate Reader (Varioskan Flash) after the cells were exposed to the tested compounds for 48 h, and the total protein content was simultaneously measured using the Bradford assay (Bio-Rad, California, USA) to normalize luminescent units.

The maximally induced level of luciferase activity that was obtained with E2 was set at 100%, and the responses of other compounds were converted to a percentage of the maximum level. The limit of quantification of the assay was 5% of the E2 max and was calculated as 3 times the standard deviation of the solvent control. Effect levels (EC_x) were determined by fitting the best regression equations to the concentration response data in the percentage

of E2 max for each compound using Sigma Plot Software. Because some compound concentration–response curves did not reach or exceed the E2 EC_{50}, the relative estrogenic potency (REP) was calculated by dividing the EC_{20} of E2 by the EC_{20} of the bisphenols. Three replicates were performed in each experiment.

Cytotoxicity assessment

The compounds were tested for their cytotoxicity towards MVLN cells using a LIVE/DEAD® Viability/Cytotoxicity Kit (L-3224) (Molecular Probes, Invitrogen, Eugene, OR). Live cells were determined using the polyanionic dye calcein, which is retained within live cells and produces an intense uniform green fluorescence under UV light (ex/em ~495 nm/~515 nm). Dead cells were identified using ethidium homodimer-1 (EthD-1) dye, which binds to occult DNA when cells are lysed, and produces a bright red fluorescence under UV light (ex/em ~495 nm/~635 nm). The labeled cells were viewed under the fluorescence microscope, and the cytotoxicity was determined by the changes of the amounts of live and dead cells (Figure S1).

Molecular docking calculations

The molecular structures of the tested ligands (Fig. 1) were sketched using SYBYL X1.2 software. Subsequent geometric optimizations were performed using Gaussian09 at the B3LYP/-cc-pVTZ level. The crystal structures of ERα in complexes with E2, BPA and BPC were used as the receptor structure (1ERE, 3UU7 and 3UUC). The missing H atoms and incomplete residues were repaired using the Biopolymer module of Sybly X1.2 software. The protonation state of the key residue His524 was set as the neutral form in which the H atom was assigned to the epsilon N of the imidazole ring.

To explore the binding modes of ligands in the binding pocket of ERα, the LeDock program (http://www.lephar.com/software.htm) was adopted to perform all docking calculations. The docking program was designed to evaluate the protein–ligand interactions and to predict their binding poses. Recent comprehensive evaluations of docking programs (AutoDock, AutoDock Vina, MOE Dock, LeDock, LigandFit, rDock, UCSF DOCK, Glide, GOLD and Surflex-Dock) indicated that LeDock has an outstanding accuracy of pose-prediction based on the PDBbind database that contains 2002 protein–ligand complexes (Wang et al. 2016). Besides, our trial suggested that LeDock made excellent performance in predicting the binding affinity of the TTR–OH-PBDEs complex (Cao et al. 2017). Utilizing the LePro module of the LeDock programs, the binding cavity was generated and was centered on the corresponding native ligand binding site for ERα with the box size

extending in x, y, and z directions and with a radius of 5 Å. To perform adequate conformational searching, we conducted 100 independent runs for each ligand. The receptor structure was kept rigid while the tested ligands were flexible throughout the process of performing docking calculations. The remaining parameters were set to default values.

Considering the computational cost, most docking studies adopted the rigid receptor and flexible ligand during the entire docking calculations. This strategy was widely used in the computational toxicology for searching the most favorable binding mode/pose of ligand in the active pocket of protein (Ren et al. 2015; Yang et al. 2017; Sheng et al. 2016). However, the opposite scenario (flexible receptor and rigid ligands) was hardly utilized because it is nearly impossible to scan the whole conformational space of a protein in a limited time, while the conformational searching of ligand structure is practical and also necessary for accurate prediction of the binding mode. In a real life, both receptor and ligand should be considered as the flexible structure for evaluating their interactions. Unfortunately, such requirement cannot be totally fulfilled by docking technique. In fact, even those so-called flexible docking methods taking the protein plasticity into account, somehow, only allow limited residues to optimizing their side chain orientation in practice (Han et al. 2013). Therefore, in order to achieve the objectives of the present study, a protein-rigid docking coupled with subsequent MD analysis was adopted. Herein, MD simulation was carried out in the current study based on the docking results of LeDock as an initial point to assess the binding stability of BPs and explore the most favorable binding mode during molecular recognition process. Such computational scenario has been proved to be rather successful in investigating the binding behavior of small molecule in the biomacromolecule, allosteric modulation of receptor and protein folding analysis (Zhao et al. 2013; Kruse et al. 2012; Metskas and Rhoades 2015).

MD simulations

According to the above docking results for the ligand-ERα complex, the NR box2 peptide (KILHRLLQE) coordinates (the chain C of 3UUD) were introduced manually into shallow activation function 2 (AF2) surfaces of ERα, which is representative of short LxxLL motifs of SRC-1 co-activators in breast cancer cells (Delfosse et al. 2012). The triple complexes of ligand-ERα-cofactor that were obtained were expected to compare with the recruitment potency of co-activator peptides upon binding of different ligands.

The Amberff14SB force field (Maier et al. 2015) was applied for protein and co-activator peptides to obtain suitable topology parameters. The partial charges of the ligands were generated by the RESP fitting method (Fox

and Kollman 1998) at the B3LYP/cc-pVTZ level, which is compatible with the general AMBER force field (GAFF) (Wang et al. 2004). Subsequently, the binary and triple complexes were added with the H atoms using the tleap module of AmberTools14 (Roe and Cheatham 2013), while the protonation states of ionizable residues were set based on the predicted result of H++ program (Anandakrishnan et al. 2012) at a physiological pH (pH 7.4). All the resulting complex systems were then solvated in a cubic water box of a TIP3P model (Jorgensen et al. 1983) with at least 10 Å of distance from the edge to the surface of the protein. Subsequently, the appropriate number of Na^+ ions was used to neutralize the entire system. The particle mesh Ewald method (Darden et al. 1993) was used to estimate long-range electrostatic interactions for periodic boundaries (cutoff = 10 Å). All R–H bonds were constrained using the SHAKE algorithm (Ryckaert et al. 1977). The integration time step was set to 2 fs using the Verlet leap-frog algorithm. To relax each system, structure minimizations containing a 2500 step steepest descent followed by a 2500 step conjugate gradient were performed with or without the restriction of a force constant $k = 100$ kcal/mol Å^{-2} on the solute. Subsequently, the entire system with the restraint $k = 10$ kcal/mol Å^{-2} for both ligand–protein and ligand–protein–cofactor complexes was heated gradually in the NVT ensemble from 0 to 300 K over 500 ps and then relaxed by a 500 ps MD simulation in the NPT ensemble for density equilibrium. Finally, a 60 ns production simulation was performed for each simulation system at 1 atm and at 300 K in an NPT ensemble. Constant pressure and temperature were maintained using a Berendsen barostat with isotropic position scaling (Berendsen et al. 1984) and a Langevin thermostat with 2 ps^{-1} collision frequency, respectively. For each restart calculation, an "ig = −1" option was set as the pseudo-random number in order to avoid a synchronization effect (Sindhikara et al. 2009). All minimizations and equilibrium MD simulations were run using the pmemd. MPI program of the AMBER12 package. The MD simulations of the production stage were implemented by a GPU-accelerated PMEMD module (Salomon-Ferrer et al. 2013) (pmemd.cuda) using the hybrid SPFP model on a single Nvidia Tesla K20 card. Trajectory coordinates were saved every 2 ps for subsequent analysis (30,000 frames per trajectory). Details regarding all simulation systems are summarized in Table S1.

Binding free energy calculations

The binding free energies were calculated using a Molecular Mechanics/Generalized Born Surface Area (MM/GBSA) approach (Hou et al. 2011a, b; Mongan et al. 2007), which was performed in a parallel algorithm in an MMPBSA.py.MPI module of AmberTools14 (Roe and Cheatham 2013). The polar solvation energy was computed using the GB model (Onufriev et al. 2004) that was developed by Onufriev et al. (igb = 2), while the non-polar solvation energy was evaluated for the solvent-accessible surface area (SASA) using the LCPO method (Weiser et al. 1999). The ionic strength (istrng) was set to 0.15 mM. Other parameters were set to default values (Miller et al. 2012). All energy components were calculated using 3000 snapshots that were extracted from the last 30 ns simulations. To identify the key residues that were responsible for the cofactor recruitment, the energy contribution of each residue was estimated using the energy decomposition module of MMPBSA.py. The entropic contribution ($-T\Delta S$) was ignored due to the low accuracy and the high cost in the prediction of the binding free energy (Cao et al. 2017).

Statistical analysis

SPSS statistical software (Version 13.0) and Sigma Plot 10.0 were used for statistical analysis. The significant differences between control and treated groups were determined using a one-way analysis of variance and Tukey's multiple range test. Differences were statistically significant if $p < 0.05$.

Results

Bisphenol compounds induce cell proliferation

The estrogenic potency of 14 bisphenols was characterized using the E-Screen bioassay to investigate their ability to induce cell proliferation in MCF-7 cells. In this cell line, the full ER agonist E2 strongly induced significant proliferation in a dose-dependent manner, with an EC$_{50}$ value of 2.68×10^{-11} M. All tested compounds increased cell proliferation in the range between 13.7 and 99.3% (1×10^{-9} M E2 was set at 100%), but their potency was very low in comparison to E2 (Fig. 2). BPAF induced 50% cell proliferation at a concentration below 5×10^{-8} M and was a strong agonist among the tested BPs. Five BPs, including BPAP, TBBPA, TBBPS, TMBPA and TCBPA induced a relative proliferation effect below 50% at all concentrations that were tested. Other BPs showed a similar estrogenic potency by inducing 50% cell proliferation in the range between 5×10^{-7} and 5×10^{-6} M.

Estrogenic activities of bisphenol compounds in a reporter gene assay

The relative estrogenic potency of 14 BPs was further determined by measuring the luciferase activity in

Fig. 2 Relative proliferation effects of 14 bisphenols in MCF-7 cells. *Number sign* The testing dilution is cytotoxic to the MCF-7 cells
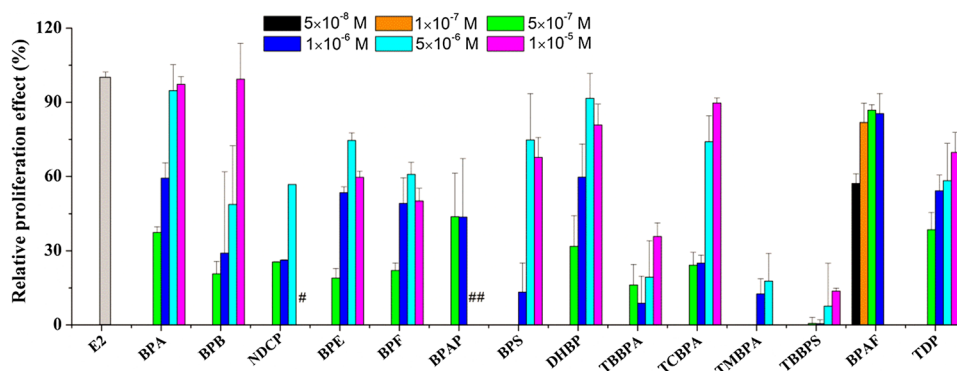

MVLN cells. Prior to the MVLN assay, the cytotoxic effect of each compound was determined using a LIVE/DEAD® Viability/Cytotoxicity Kit. BPAP exhibited significant cytotoxicity in MVLN cells at 1×10^{-5} M (Figure S1). TCBPA, TBBPA and TBBPS produced significant cytotoxicity in MVLN cells at 5×10^{-5} M. Exposure of MVLN cells to other bisphenols did not produce significant cytotoxicity in a concentration range up to 5×10^{-5} M, and no cytotoxic effects were observed by microscopic examination (data not shown). A concentration–response curve was developed for all BPs up to 5×10^{-5} M, and the luciferase activity behaved differently, depending on the compound tested. As shown in Fig. 3, the luciferase activity induced by TCBPA, TBBPA and TBBPS was at a basal level (<5%). Therefore, their relative estrogenic potencies (REP) could not be determined (Table S2). Four BPs, including NDCP, BPB, BPAP and TDP induced a luciferase activity below 50%, whereas BPA, BPE, BPF, BPS, BPAF and DHBP induced a luciferase activity greater than 50% in a dose-related manner. BPAF induced a 50% relative luciferase activity at a concentration between 1×10^{-6} and 5×10^{-6} M and was a strong agonist among the bisphenols that were tested. The REP for each BP was calculated by dividing the EC_{20} for E2 by the EC_{20} for the BP (Table S2). BPAF had the highest estrogenic activity, followed by BPS, DHBP, BPE, BPF, BPA, TMBPA, BPB, TDP, BPAP and NDCP. TBBPA, TCBPA and TBBPS produced no estrogenic activity in the MVLN assay.

As a high affinity ER antagonist, the effect of ICI 182,780 was to inhibit the nucleocytoplasmic shuttling of the receptor by blocking its nuclear uptake. In this study, ICI 182,780 (10 nM) was co-exposed to MVLN cells with BPs at the highest induction concentration, which was obtained from the MVLN assay. As shown in Fig. 4, co-exposure of ICI 182,780 with the tested BPs resulted in complete inhibition of luciferase activity, indicating that these compounds exhibited estrogenic activity by activating the ER in the MVLN assay.

## Bisphenols interact with ERα in molecular docking simulations

To gain structural insights into the binding mode of the tested bisphenols to ERα, we employed the LeDock program to predict the interaction patterns of these ligands at the E2 binding site of ERα. Before conducting docking simulations, we first evaluated the predicted accuracy of the current docking program by evaluation of the sampling power on the ERα-ligand complex system. The ability to reproduce the native binding pose is defined as the sampling power of a docking tool. In the current study, the root-mean-square deviation (RMSD) values for 73 known crystal complexes between the top scored ligand binding poses and the native ligand binding poses were calculated and are tabulated in Table S3. If the RMSD for one redock calculation was less than a threshold of 2.0 Å, a success was recorded. Finally, the overall success rate of different docking programs was calculated as the sampling power. Among the docking tools that were tested, LeDock exhibited a satisfactory performance in the prediction of a native ligand pose with the highest success rate (0.88). Hence, based on the above evaluation, we adopted the LeDock program to predict the binding modes of the tested bisphenols to ERα.

By comparing the crystal structures of ERα in complex with BPA, BPAF and BPC, we found that the three ligands displayed different binding poses in the ligand-binding pocket of ERα (Figure S2). BPA acted as the natural agonist E2 and induced the agonist-bound conformation, in which H12 covers the LBD pocket, whereas BPC triggered the repositioning of H12 into the ERα surface groove and adopted a similar LBD conformation that was induced by the typical antagonist OHT. In particular, BPAF exhibited two distinct poses in separate monomers of the ERα dimer, which were defined as BPAF-A (BPC-like mode) and BPAF-B (BPA-like mode) (Figure S2). In comparison with BPAF, BPC possesses the double bond C=C for retaining relative structural rigid, which forms more stable hydrogen bonding interactions with Thr347. The experimental data also
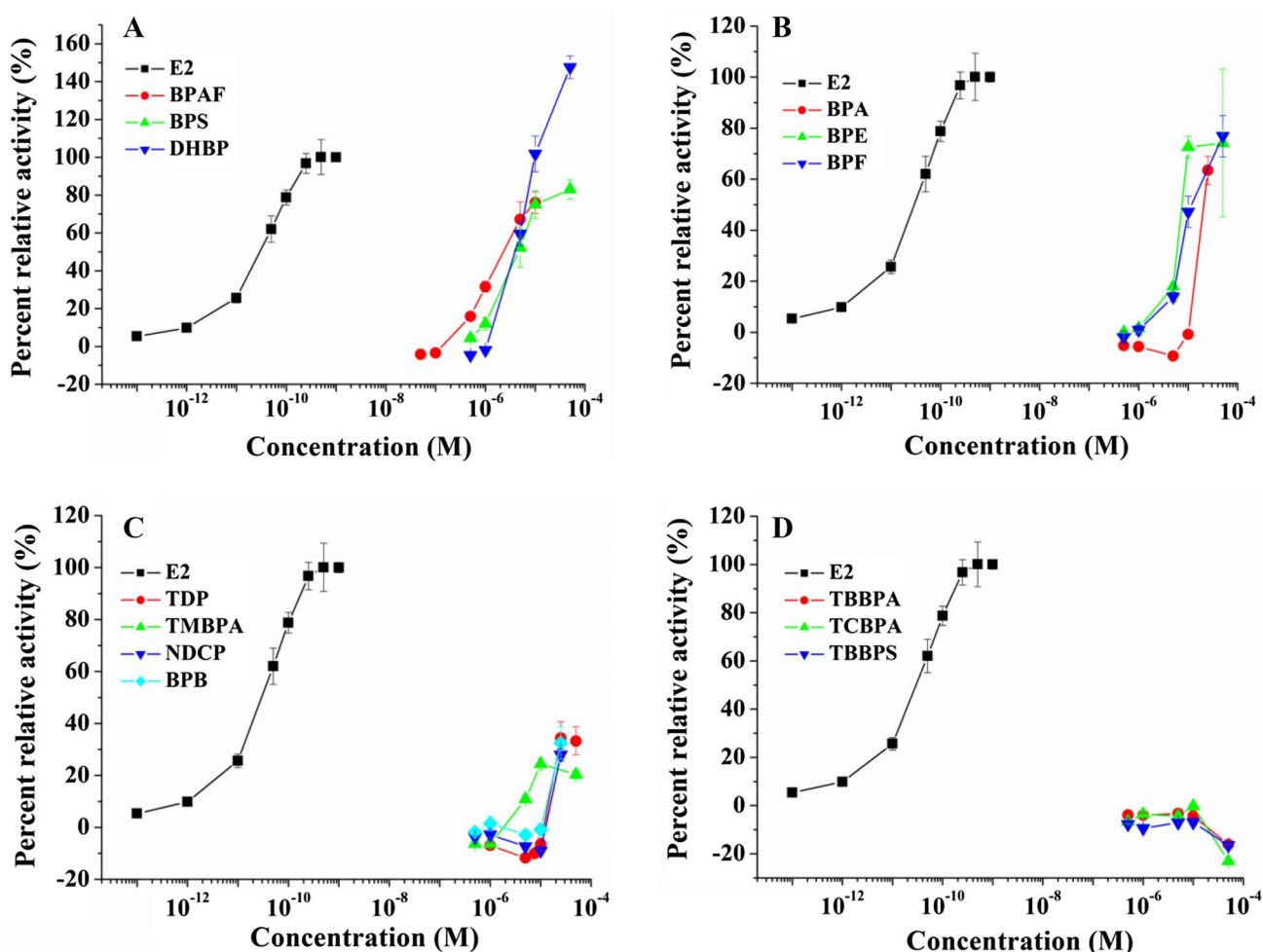
Fig. 3 Dose–response curves for 14 bisphenols in MVLN cells. **a** Relative estrogenic activity of BPAF, BPS, and TMBPA; **b** relative estrogenic activity of BPA, BPE, and BPF; **c** relative estrogenic activity of TDP, TMBPA, NDCP and BPB; **d** Relative estrogenic activity of TBBPA, TBBPA, and TBBPS. The maximal luciferase activity (100%) was obtained with 1 nM E2
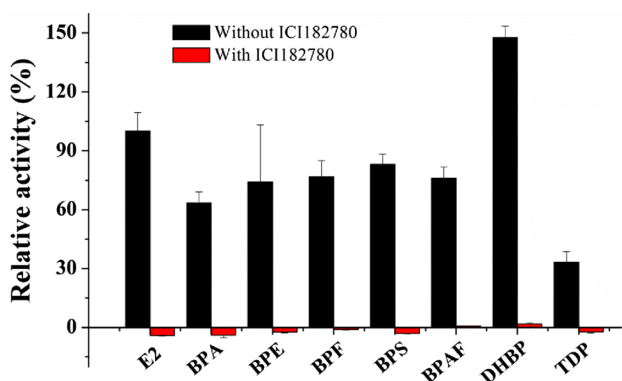
Fig. 4 Relative inhibition activity in luciferase assay when co-exposure of ICI 182,780 with the tested bisphenols

indicated that BPC has stronger ERα binding affinity than BPAF does (Delfosse et al. 2012). The ability of a ligand to interact with Thr347 via hydrogen bond seems to be an important element for its stable binding to ERα, esp. for the antagonist. Furthermore, within the above binding modes, residue Thr347 exhibited two different side chain dihedral angles χ1 (N-CA-CB-CG2) in a key recognition position, thereby causing the different structural characteristics upon ligand binding into the active pocket of ERα. For instance, when the –OH group of Thr347 points to the external part of the binding pocket, BPA and BPAF-B are close to residue His524 because of H-bonding interactions. In contrast, BPC and BPAF-A form H-binding interactions with Thr347 by means of the inward orientation of the –OH group.

Therefore, to compare the effects of the conformational changes that involve the side chain of Thr347 during the ligand recognition process, we docked all the tested bisphenols into three receptor structures (3UU7, 3UUC and 1ERE) that have different Thr347 conformations. By comparing the key interactions between ERα and 14 BPs based on the superimposition of the docking pose, we found that both BPA-like and BPC-like modes existed in the binding pocket of ERα. In the 3UU7 results (Fig. 5a), all binding poses of ligands adopted the BPA-like mode without H-bonding interactions with Thr347 due to the external orientation of the side chain (dihedral angle of 296.0°). Besides, the docking results showed that the hydrogen bonds between the –OH on the phenolic group and the N^δ atom on the imidazole moiety of His524 were established for BPA, BPAF, BPF, BPS, DHBP and TDP, which were marked with green dash line in Fig. 5. For the other ligands, the H-bonding interactions were not observed.

Conversely, in the 3UUC results (Fig. 5b), the inward orientation of Thr347 prompted the ligands to form H-bonding interactions with the –OH group of the side chain (dihedral angle of 175.9°). Interestingly, Thr347 shows a $\chi1$ of 118.5° in the 1ERE structure, which was considered as a semi-stable conformation between 3UUC ($\chi1 = 296.0°$) and 3UU7 ($\chi1 = 175.9°$). This conformation results in a different recognition preference for Thr347 or His524 in the predicted binding modes of the tested bisphenols. Some bisphenols, such as BPAP, BPE, BPF, TBBPA

and TBBPS, may form H-bonding interactions with neither Thr347 nor His524. Furthermore, we also observed that only TCBPA could form solid H-bonding interactions with Thr347 in the 1ERE structure, while other compounds form H-bonding interactions with His524 (Fig. 5c). Therefore, based on the above docking results, the conformation of Thr347 is proposed to play a key role in the recognition of the bisphenol compounds. To decipher the recognition mechanism involving the structurally dynamic changes of Thr347 at the E2 binding site of ERα, the above binding modes in the 1ERE structure were explored further and clarified by MD simulations.

MD simulations investigate the dynamic binding process

The root-mean-square deviation (RMSD) values for protein Cα atoms were calculated to assess the convergence of simulation systems of ERα complexes that were bound by the tested bisphenols. As shown in Figure S3, all simulation systems exhibited an increasing fluctuation in the initial 3 ns simulation and reached equilibrium phases with RMSD at ~1.5 Å after 20 ns of MD simulations, suggesting that the simulation systems were stable throughout the explicit water environment.

Further H-bonding analysis demonstrated that by the formation of H-bonding interactions with Glu353
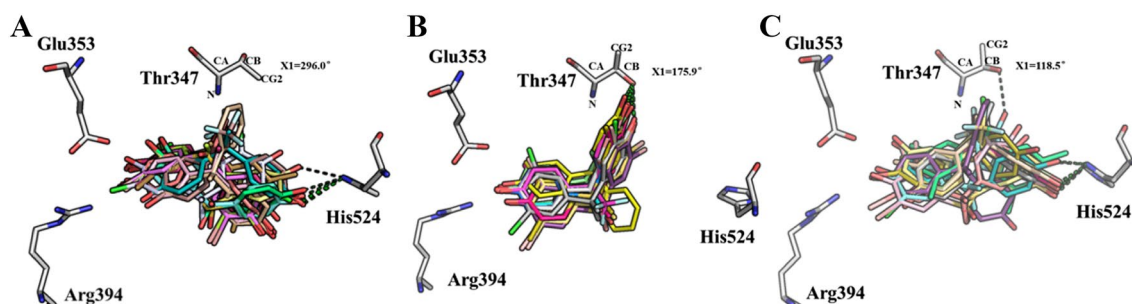
Fig. 5 Docking pose alignment in the 3UU7 (**a**), 3UUC (**b**) and 1ERE (**c**) structures for 14 bisphenols

Fig. 6 H-bonding occupancies of tested compounds with His524 (*black bar*), Glu353 (*red bar*) and Thr347 (*blue bar*) during 60 ns MD simulation process (color figure online)
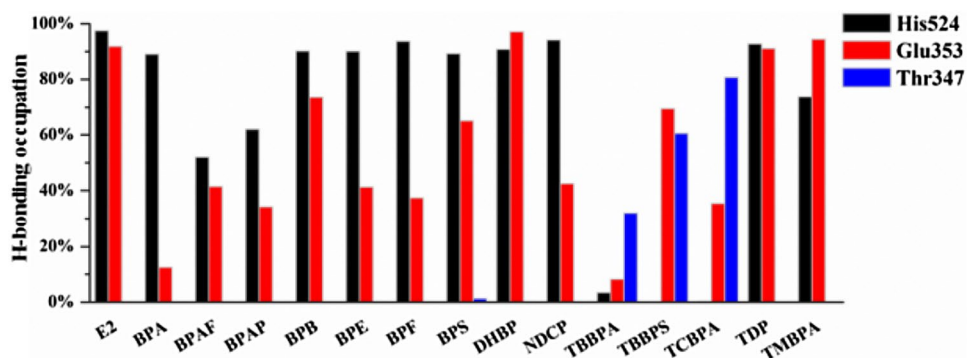
and His524, most of the ligands hold the binding mode of BPA-like for 60 ns except for TCBPA, TBBPA and TBBPS (Fig. 6). With respect to TBBPA and TBBPS, the induced-fit torsion of the Thr347 side chain was present in the early stage of MD simulation. As shown in Fig. 7, we delineated the evolution of distance between TBBPA and Thr347 or His524 for the TBBPA-ERα simulation system. First, one phenol ring of TBBPA wraps around His524 at a distance of 3.7 Å at the initial point of the simulation (0 ns). As the simulation time increased, a dynamic recognition process was observed in the binding of TBBPA, which exhibited alternative H-bonding interactions with Thr347 or His524 at the beginning stage of the simulation (0–13 ns). Subsequently, TBBPA moves away from His524 and gets closer to Thr347, displaying a stable recognition state. The newly formed H-bond between Thr347 and BPC can hold tightly until the end of the simulation. Similarly, TBBPS also displayed a dynamic recognition process and finally formed an H-bond with Thr347 for ~46 ns, while TCBPA suffers a transient dynamic recognition and a long stable H-binding interaction with Thr347 for ~59 ns (Figure S4). Based on the analysis of the binding process, we inferred that TCBPA TBBPA and TBBPS may prefer the BPC-like binding mode rather than a BPA-like one.

Stability of H12 and loop H11–H12 upon the binding of bisphenols

Subsequently, the stability of H12 was investigated because the repositioning of H12 plays a significant role in the transcriptional activity of ERα. To explore the effects of the tested bisphenols on the structural characteristics of ERα, the time profiles of RMSD for H12 and the loop structure contacting H11 and H12 in each system were calculated after the mass-weight aligning of ERα LBD (Figure S5). A low RMSD with small amplitude implies that the corresponding structure becomes stable, while a high RMSD with large amplitude implies that the structural coordinates move away from the initial positions. The averaged RMSDs during the last 40 ns of simulation were calculated for each system in Figure S5. It should be noted that the RMSD value for H12 and loop H11–H12 in the TCBPA-ERα system reached 3.82 ± 0.57 Å, which is obviously higher than the other simulation systems, indicating that the movement of H12 in the TCBPA-ERα system was not stable. Moreover, TBBPA-ERα, TBBPS-ERα and NDCP-ERα have high RMSD values of 3.00 ± 0.29, 2.90 ± 0.34 and 3.01 ± 0.26 Å, respectively, implying that the fluctuations of H12 in these systems were larger relative to that in the E2-ERα system (2.70 ± 0.33 Å). We also found

Fig. 7 Dynamic binding process of TBBPA during 60 ns MD simulation
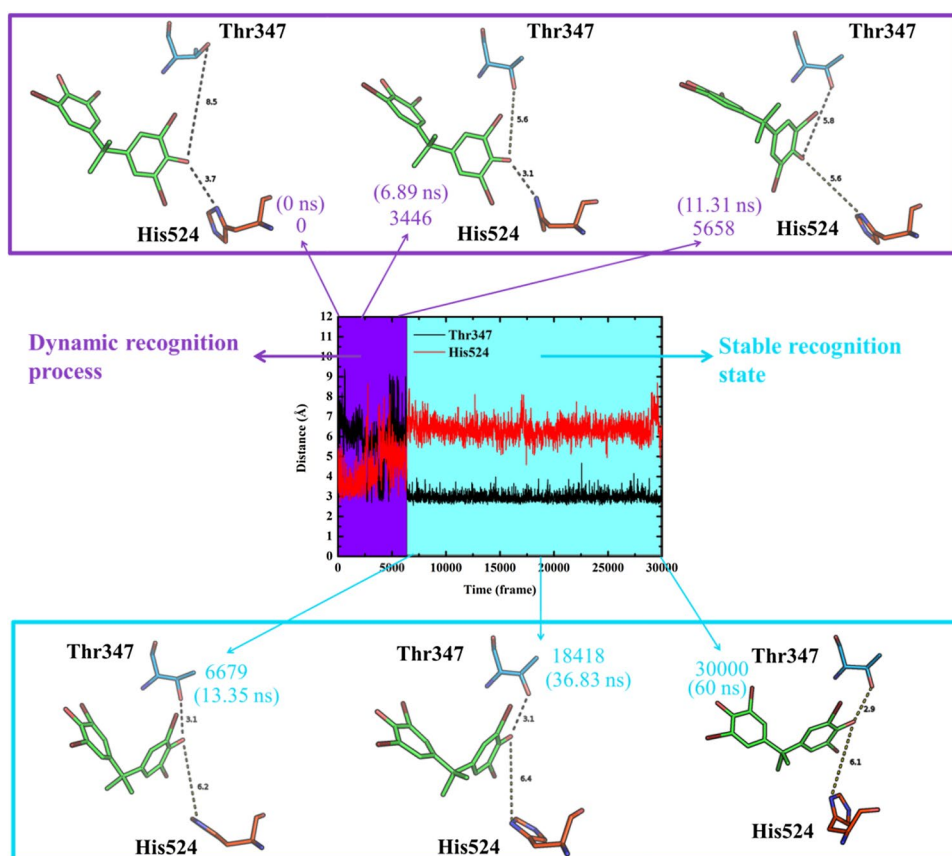
that compared to the E2-ERα system, a comparable averaged RMSD was detected in ligand-bound complexes for BPA, BPAF, BPAP, BPB, BPE, BPF, BPS, DHBP, TDP and TMBPA (Figure S5), suggesting that the conformational changes of Loop H11–H12 and H12 have relatively small deviations from the initial agonist position in these systems.

To evaluate the contributions of the BPs to the conformational changes of H12 when binding to ERα, the representative conformation during the 20–60 ns MD simulation for each system was obtained by the average-linkage clustering algorithm using the cpptraj module of Amber-Tools14. All the dry trajectories of ligand-ERα complexes without water molecules and Na$^+$ were partitioned into the 3 distinct clusters. The conformations of the first and second clusters were then extracted as representatively simulated structures. Figure 8 displays the alignment results for the 1ERE crystal structure that was used as the initial MD point and the representative conformations of E2-ERα, BPAF-ERα and TCBPA-ERα complexes during the MD simulation process. Clearly, the representative MD conformations of E2-ERα exhibited a small deviation from the 1ERE structure, implying that the H12 and loop H11–H12 structures are stable and reliable compared to the corresponding crystal result for the E2 binding (Fig. 8a).

Furthermore, we observed slight structural changes in the end part of H11 (Met528-Lys531) for the BPAF-ERα complex by superimposition of the MD structure with 1ERE (Fig. 8b). The result suggests that BPAF can activate ERα partly by stabilizing the H12 structure in the agonist-bound conformation. Similar results also were obtained with BPA, BPAF, BPAP, BPB, BPE, BPF, BPS, DHBP, TDP and TMBPA. However, the shift in part structures of H11 and loop H11–H12 was found in the representative conformation of the top cluster denoted as C1 with 72.6% occupancy, thereby leading to the unusual drift of the H12 structure (Fig. 8c). Likewise, deformation of the H12 structure occurs in the representative conformation of the second cluster denoted as C2 with an occupancy of 21.1%, indicating that TCBPA may induce an unstable H12 motion (Fig. 8d). The representative structures of the TBBPA-ERα, TBBPS-ERα and NDCP-ERα systems that are based on clustering analysis partly exhibit the structural features that are similar to the TCBPA-induced conformation. As reported in the previous study, the stable conformation of H12 in the agonist-bound conformation is crucial to the recruitment of the co-activator. Thus, we speculated the bisphenol-induced conformational changes could affect the binding of activation cofactor to ERα by stabilizing the H12 position.

Impact of BPs on the binding of co-activator to ERα

When a ligand binds to ERα, its induced allosteric modulation can facilitate or impede the subsequent recruitment of cofactors in the shallow groove of the ERα surface. Therefore, to better understand the allosteric effects of BPs on the regulation of binding of SRC-1 NR2 peptides at the AF2 surface of ERα, we investigated the ability of

Fig. 8 Representative conformations of E2-ERα (**a**), BPAF-ERα (**b**) and TCBPA-ERα (**c**, **d**) complexes during 60 ns MD simulation process
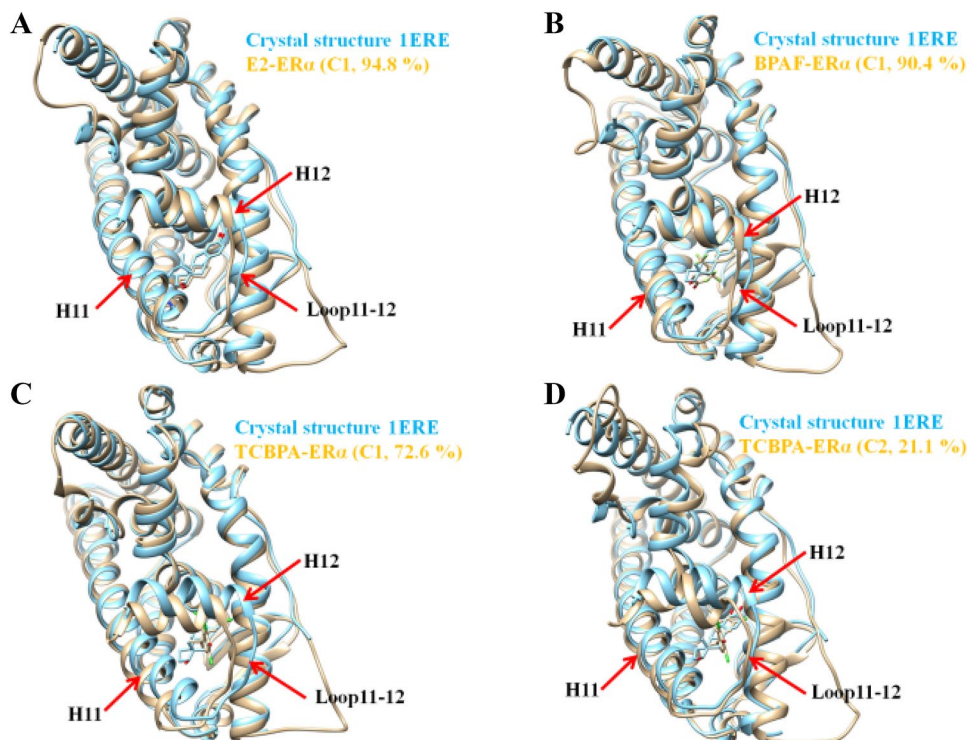
co-activator recruitment by conducting MD simulations of the triple complex systems (ligand-ERα-cofactor). From the calculations of the free energy of binding between co-activator peptides (KILHRLLQE) and ERα, we found that the E2-ERα-cofactor system exhibited the highest binding affinity for co-activator peptides (−53.35 kcal/mol). The remaining systems exhibited decreased binding affinities from −46.21 to −40.41 kcal/mol as follows: BPA, BPAF, BPAP, BPB, BPE, BPF, BPS, DHBP, NDCP, TDP and TMBPA (Table 1). These results implied that the ERα complexes bound to bisphenols were not stable relative to the E2-bound complex, and reduced the co-activator recruitment in virtue of the ligand-induced allosteric modulation. Moreover, TBBPA, TBBPS and TCBPA displayed the worst binding affinities for co-activator recruitment in the current MM-GBSA calculations (−38.71, −38.47 and −35.05 kcal/mol, respectively), implying that the ligand induced significant interface with the binding of co-activator in the AF2 surface of ERα. During the MD simulation processes, the three compounds retain the BPC-like binding mode through stable H-binding interactions with Thr347, suggesting that this ligand binding mode may be a major factor in reducing their estrogenic activities in the MVLN assay by an allosteric effect on the co-activator recruitment of ERα.

Discussion

BPs, which consist of two phenolic rings joined together by a bridging carbon or other chemical structures, are structurally similar to BPA. BPA has been identified as a weak estrogenic chemical that modifies natural endocrine functions through binding to the estrogen receptor. However, until recently, little attention has been paid to the estrogenic activity of other BPs. Because of their similar molecular structures and physicochemical properties, BPs may also exhibit similar toxicological effects. Kitamura et al. (2005) compared the endocrine-disrupting activities of BPA and 19 related compounds by means of different in vitro and in vivo reporter assays, and observed remarkable differences in their estrogenic activities. Our recent work demonstrated that exposure to TCBPA, TBBPA and BPAF resulted in developmental toxicity in zebrafish embryos/larvae, but only BPAF specifically exhibited estrogenic activity (Song et al. 2014). Moreover, some of these chemicals, such as BPA, BPF, BPS, TBBPA, and TCBPA, have been detected in human blood (Jakobsson et al. 2002; Andrianou et al. 2016; Liu et al. 2017), indicating that these chemicals are humans actually exposed or represent an actual health threat.

In the present study, the tested BPs varied in their estrogenic potency and efficacy. BPAF exhibited the highest estrogenic activity in both the MVLN assay and the E-screen assay. Most of the tested BPs exhibited a relative potency similar to BPA, whereas TBBPA, TCBPA and TBBPS produced no measurable luciferase activity in the MVLN assay (Table S2). However, an effect on cell proliferation by TBBPA, TCBPA, and TBBPS was observed in the E-screen assay. As far as we know, the E-screen assay has an intrinsic limitation: that a positive response cannot be attributed strictly to estrogen receptor agonists. Previous studies have demonstrated that a range of non-estrogenic substances, including androstenediol, progesterone, epidermal growth factor, insulin-like growth factors, caffeine and ethanol, can influence the proliferation of human breast

Table 1 Binding free energy of co-activator recruitment in the ligand-ERα-cofactor complex systems (unit: kcal/mol)

Systems	ΔE_{vdw}	ΔG_{SA}	ΔE_{ele}	ΔG_{GB}	ΔG_{cal}
E2-ERα-cofactor	−51.66 (4.53)	−8.92 (0.43)	−647.43 (42.19)	654.65 (38.92)	−53.35 (5.16)
BPA-ERα-cofactor	−48.36 (4.85)	−8.10 (0.68)	−570.38 (66.25)	580.63 (64.99)	−46.21 (5.96)
BPAF-ERα-cofactor	−44.65 (4.07)	−7.27 (0.49)	−501.73 (47.83)	511.26 (45.59)	−42.40 (5.05)
BPAP-ERα-cofactor	−45.54 (4.05)	−7.50 (0.47)	−552.00 (40.71)	562.83 (40.65)	−42.22 (3.98)
BPB-ERα-cofactor	−45.06 (4.39)	−7.37 (0.63)	−527.71 (61.38)	539.42 (58.67)	−40.73 (6.15)
BPE-ERα-cofactor	−45.44 (4.16)	−7.66 (0.46)	−585.54 (43.25)	595.01 (41.61)	−43.64 (4.51)
BPF-ERα-cofactor	−45.83 (4.12)	−7.54 (0.57)	−549.71 (61.46)	561.57 (60.19)	−41.50 (4.77)
BPS-ERα-cofactor	−47.81 (4.22)	−7.97 (0.54)	−580.36 (45.30)	591.49 (43.79)	−44.65 (4.98)
DHBP-ERα-cofactor	−43.99 (4.14)	−7.05 (0.51)	−507.25 (50.94)	516.35 (49.95)	−41.93 (5.10)
NDCP-ERα-cofactor	−45.87 (4.37)	−7.60 (0.58)	−562.44 (52.18)	572.76 (50.61)	−43.16 (5.19)
TBBPA-ERα-cofactor	−42.05 (3.96)	−6.89 (0.53)	−540.83 (63.45)	551.06 (61.55)	−38.71 (5.02)
TBBPS-ERα-cofactor	−42.55 (5.08)	−7.05 (0.71)	−512.23 (66.81)	523.36 (65.02)	−38.47 (6.08)
TCBPA-ERα-cofactor	−41.30 (4.25)	−6.62 (0.62)	−480.11 (77.08)	492.99 (74.92)	−35.05 (5.39)
TDP-ERα-cofactor	−45.02 (4.82)	−7.42 (0.73)	−514.21 (84.00)	524.74 (83.20)	−41.91 (5.71)
TMBPA-ERα-cofactor	−45.02 (4.16)	−7.32 (0.62)	−529.29 (70.63)	541.22 (67.84)	−40.41 (6.08)

$\Delta G_{\text{cal}} = \Delta E_{\text{vdw}} + \Delta G_{\text{SA}} + \Delta E_{\text{ele}} + \Delta G_{\text{GB}}$. Standard error of mean values is displayed in parenthesis

cancer cells (Ando et al. 2002; Dickson and Lippman 1995; Diel et al. 1999; Osborne et al. 1990; van der Burg et al. 1988). Furthermore, the E-screen assay might be extremely sensitive to small changes in the physical or chemical properties of culture conditions that are induced by test substances, leading to non-specific increases or decreases in proliferation independent of ER-binding (Desaulniers et al. 1998). In this study, we used an anti-estrogen, ICI 182,780, to distinguish estrogenic from non-estrogenic activity. There was a full reduction in luciferase activity when ICI 182,780 was exposed to E2 and the tested BPs in the MVLN assay, indicating that BPs induced luciferase by activating ER (Fig. 4). However, ICI 182,780 could partially inhibit the cell proliferation that was induced by TCBPA in an E-screen assay (data not shown), indicating that this positive response cannot be attributed strictly to estrogen receptor agonists.

The estrogenic potencies of the eight BPs that were identified in sewage sludge were evaluated using a bioluminescence yeast estrogen screen (BLYES) assay in our recent work (Ruan et al. 2015). All the tested BPs exhibited estrogenic activity in the BLYES assay, but there were significant differences in the potencies of the individual chemicals. Furthermore, the crystal structures of ERα in complex with BPA, BPAF and BPC have been reported previously by Delfosse et al. (2012), and indicated that the ligands displayed quite different binding poses in the ERα LBD (Figure S2). However, the static crystal structures could not offer details about the dynamic binding process, or structural characteristics involved in the allosteric modulation for the recruitment of co-activator. A better understanding of the detailed binding mechanisms for these compounds in the ERα LBD requires further study. Alternatively, the previous use of the ERα-Y537S LBD mutant for crystallizations (Delfosse et al. 2012) enhanced the stability of H12 in the agonist conformation, and further facilitated the constitutive activation for transcriptional activity of ERα in the absence of ERα agonists (Robinson et al. 2013). Thus, the obtained crystal complexes of ligand-ERα-Y537S might significantly reinforce the strength of ligand-ERα interactions, which might not be suitable as an initial model to study the subsequent allosteric modulation of the recruitment of co-activator.

Therefore, we employed a computational strategy that combined molecular docking with MD simulations to explore the recognition mechanism of 14 BPs upon binding with wild type ERα, which is a major receptor subtype for estrogenic activity to control the response of the binding of endogenous and exogenous molecules. Based on the docking results of the LeDock program, we found that the docking tool could provide a reasonably predicted binding pose of ligands by comparing the known crystal structures. Furthermore, the logarithm of

the relative binding affinity of ligands (logRBA) of a compound compared with E2 was extracted from a previous report (Ng et al. 2015). As shown in Table S4, the correlation coefficient between the docking score and the experimental logRBA for nine compounds is summarized for three ERα structures (one wild type and two mutant structures). By comparing the correlation coefficients, we found that using the 1ERE structure as a docking template for the receptor, the predicted binding scores correlated with the experimentally determined binding affinities of the ligands ($R^2 = 0.66$, $p < 0.001$), indicating that the docking score based on the 1ERE structure could be used to assess the binding affinities of other bisphenol compounds with ERα. The predicted results indicated that BPAF, BPAP, BPB, BPE, BPF, BPS, DHBP, NDCP, TDP and TMBPA have comparable affinities for ERα relative to BPA. In particular, BPAF exhibited the highest binding affinity among the above compounds in terms of a predicted score (-5.86 kcal/mol), which is in accordance with the observed estrogenic activities in the MVLN assay. It should be noted that these compounds are similar to BPA with minor structural differences and, therefore, can export weak estrogenic activities. At the same time, we also found that compounds having an additional $-CH_3$ group in the common bisphenol skeleton, such as NDCP and TMBPA, show decreased estrogenic activities when compared with BPA. The reason behind this phenomenon was hypothesized to be that the structural change does not mimic the phenol ring function of E2 in the binding pocket for receptor stability. Moreover, substitutions of bridging carbons with different extents appear to complicate their estrogenic activities, which is in line with the obtained comparable docking scores (range from -5.86 to -4.93 kcal/mol). For example, the replacement of the $-C(CH_3)_2$ group of BPA with $-C(CF_3)_2$ or $-SO_2$ groups will increase the molecular polarity in the bridging motif, thus leading to increased estrogenic activity for BPAF and BPS. The introduction of large substituent group such as $-CH_2CH_3$ or $-Ph$ in the bridging carbon atom increases the molecular size, thereby lowering the estrogenic activities for BPB and BPAP relative to BPA. Conversely, compared to BPA, small substituent groups ($-CHCH_3$ or $-CH_2$) result in an improvement of the estrogenic activities of BPE and BPF, but not TDP. Additionally, most of the BPs that were tested as partial agonists were observed to form relatively weak H-bonding interactions with His524 or Glu353 compared to the native ligand E2 (Fig. 6), and thus were deduced to generate a mixed population of active and inactive conformations which do not accelerate completely co-activator interactions, therefore, explaining reduced transactivation responses and signaling differences. Collectively, our results demonstrated that the endocrine disruption

toxicity of these BPA substitutes should be considered with extra caution to protect public health during their production and use.

Actually, the docking analysis performed in the study showed that the ERα binding of TBBPA, TBBPS and TCBPA is more favorable than other tested BPs without halogenation on their phenyl ring, and thus present higher docking scores (Table S4). The possible reason is that the halogen substituents in the phenolic group of the molecule scaffold may increase van der Waals interactions between the ligands and the surrounding hydrophobic residues in the binding pocket. However, increased number of halogen atom on the phenyl ring, at the same time, also results in a large molecule volume and thereby leads to a rising intermolecular collision with surrounding bulky residues since the receptor was kept as the rigid structure in docking setting. TBBPA, TBBPS and TCBPA may be a bad ligand to ERα if the unfavorable collisions become important. Therefore, false positive, that a bad ligand is recognized as good one, may emerge. In other words, TBBPA, TBBPS and TCBPA may be wrongly predicted to be good ligands by the docking analysis used in the manuscript. Fortunately, subsequent MD simulation, which allows the protein to exhibit its flexibility, could be used to verify the results of LeDock. The dynamic binding process analysis indicated that during the initial stage of MD simulations, ERα endure the conformation adjustments of the three ligands with halogenation on the phenyl ring and then remained the stable conformation until the end (Figs. 7, S4).

Furthermore, after ligand binding in ERα LBD, the allosteric effect on the binding of co-activators was a crucial step for triggering subsequent gene expression. Several studies focused on the potency of co-activator recruitment for different ligands (Aarts et al. 2013; Bourgoin-Voillard et al. 2010; Bramlett and Burris 2002; Carraz et al. 2009; Jeyakumar et al. 2011; Margeat et al. 2001). Specifically, experimental results (Hanson et al. 2012) revealed that no recruitment was observed in the absence of ligand or even in the presence of E2 derivatives with a large bulky group in the C-11 position. The study of Bourgoin-Voillard et al. (2010) also demonstrated that bisphenol and its analogs exhibited antagonistic behavior by preventing the binding to LxxLL-containing peptides in the surface groove of ERα LBD. A similar study indicated that the binding affinities of probe ligands are not correlated with their potencies for co-activator recruitment or cellular ERE-reporter activations (Jeyakumar et al. 2011). Therefore, the co-activator recruitment potency of the three compounds might be lower than for other tested ligands. Subsequent MD simulations further confirmed that the binding of TCBPA could induce a structural change in ERα by shifting H11 and destabilizing H12 (Fig. 8). Furthermore, the ability to recruit the co-activator also was demonstrated to be decreased in the binding

free energy calculations for TBBPA, TBBPS and TCBPA compared to other compounds that were tested in the ternary ligand-ER-cofactor complex systems (Table 1).

Moreover, during the binding process, the induced-fit torsion of the Thr347 side chain enables the ligand to interact with it by H-bonding formation. This binding mode is similar to that of BPC which can induce the antagonist-bound conformation of ERα. Thus, we believe that the BPC-like binding mode is likely to produce anti-estrogenic activities with bisphenol compounds, while the BPA-like binding mode renders it feasible to generate estrogenic activities in terms of an induced agonist-bound conformation, which is in line with the present biophysical data (MVLN assay and MCF-7 cell proliferation). Our computational simulations further confirmed that the dynamic nature of ligand recognition is coupled to H12 stability and subsequent co-activator recruitment (Figs. 7, 8) and, therefore, implies a dynamic ensemble of binding modes which induce different proportions of active versus inactive ERα conformations in the recognition process. Similarly, this fact was previously highlighted in the derivatives of WAY-166916 that displayed multiple binding poses of ligands in the ERα crystal complex structures and, therefore, elicited a graded signaling output (Bruning et al. 2010).

Conclusions

The estrogenic potency of 14 BPs was investigated systematically in the current study by the E-Screen bioassay in MCF-7 cells and by luciferase activity in MVLN cells. In the tested BPs, BPAF showed the highest estrogenic activity, followed by BPS, DHBP, BPE, BPF, BPA, TMBPA, BPB, TDP, BPAP and NDCP. However, TBBPA, TCBPA and TBBPS exhibited no estrogenic activity in the MVLN assay, while they induced a lower proliferation of MCF-7 cells relative to other tested compounds. To further elucidate the underlying molecular basis of the binding of different BPs to ER, cumulative 1.8 μs MD simulations were performed to investigate the dynamics-based structural basis during ligand recognition processes. An H-bonding interaction with Thr347 was identified as an important structural feature for the recognition of TBBPA, TCBPA and TBBPS at the E2 binding site of ERα. Subsequent allosteric modulations resulted in a decreased stability of H12 compared to other BPs. Further assessments of co-activator recruitment suggested that the binding of the three compounds leads to weakened affinities for co-activator compared to other tested compounds, which is correlated with the estrogenic activities. Taken together, current experimental and computational results provide deep insights into the ligand-induced transcriptional activity

of ERα for 14 BPs compounds with different molecular structures.

Compliance with ethical standards

Conflict of interest The authors' declares that they have no conflict of interest.

References

Aarts JM, Wang S, Houtman R et al (2013) Robust array-based coregulator binding assay predicting ERα-Agonist potency and generating binding profiles reflecting ligand structure. Chem Res Toxicol 26(3):336–346

Anandakrishnan R, Aguilar B, Onufriev AV (2012) H++ 3.0: automating pK prediction and the preparation of biomolecular structures for atomistic molecular modeling and simulations. Nucl Acid Res 40(W1):W537–W541

Ando S, De Amicis F, Rago V et al (2002) Breast cancer: from estrogen to androgen receptor. Mol Cell Endocrinol 193(1):121–128

Andrianou XD, Gängler S, Piciu A, Charisiadis P, Zira C, Aristidou K, Piciu D, Hauser R, Makris KC (2016) Human exposures to bisphenol A, bisphenol F and chlorinated bisphenol a derivatives and thyroid function. PLoS One 11(10):e0155237

Berendsen HJ, Postma JPM, van Gunsteren WF, DiNola A, Haak J (1984) Molecular dynamics with coupling to an external bath. J Chem Phys 81(8):3684–3690

Bourgoin-Voillard S, Gallo D, Laïos I et al (2010) Capacity of type I and II ligands to confer to estrogen receptor alpha an appropriate conformation for the recruitment of coactivators containing a LxxLL motif—relationship with the regulation of receptor level and ERE-dependent transcription in MCF-7 cells. Biochem Pharmacol 79(5):746–757

Bramlett KS, Burris TP (2002) Effects of selective estrogen receptor modulators (SERMs) on coactivator nuclear receptor (NR) box binding to estrogen receptors. Mol Genet Metab 76(3):225–233

Bruning JB, Parent AA, Gil G et al (2010) Coupling of receptor conformation and ligand orientation determine graded activity. Nat Chem Biol 6(11):837–843

Brzozowski AM, Pike AC, Dauter Z et al (1997) Molecular basis of agonism and antagonism in the oestrogen receptor. Nature 389(6652):753–758

Cao H, Sun Y, Wang L, Zhao C, Fu J, Zhang A (2017) Understanding microscopic binding mechanism of hydroxylated and sulfated polybrominated diphenyl ethers with transthyretin by molecular docking, molecular dynamics simulations and binding free energy calculations. Mol Biosyst 13:736–749

Carraz M, Zwart W, Phan T, Michalides R, Brunsveld L (2009) Perturbation of estrogen receptor α localization with synthetic nona-arginine LXXLL-peptide coactivator binding inhibitors. Chem Biol 16(7):702–711

Chang C, Norris JD, Grøn H et al (1999) Dissection of the LXXLL nuclear receptor-coactivator interaction motif using combinatorial peptide libraries: discovery of peptide antagonists of estrogen receptors α and β. Mol Cell Biol 19(12):8226–8239

Chen MY, Ike M, Fujita M (2002) Acute toxicity, mutagenicity, and estrogenicity of bisphenol-A and other bisphenols. Environ Toxicol 17(1):80–86

Darden T, York D, Pedersen L (1993) Particle mesh Ewald: an N·log (N) method for Ewald sums in large systems. J Chem Phys 98(12):10089–10092

Delfosse V, Grimaldi M, Pons JL et al (2012) Structural and mechanistic insights into bisphenols action provide guidelines for risk assessment and discovery of bisphenol A substitutes. Proc Natl Acad Sci USA 109(37):14930–14935

Delfosse V, Grimaldi M, Cavailles V, Balaguer P, Bourguet W (2014) Structural and functional profiling of environmental ligands for estrogen receptors. Environ Health Perspect 122(12):1306

Desaulniers D, Leingartner K, Zacharewski T, Foster W (1998) Optimization of an MCF7-E3 cell proliferation assay and effects of environmental pollutants and industrial chemicals. Toxicol In Vitro 12(4):409–422

Dickson RB, Lippman ME (1995) Growth factors in breast cancer. Endocr Rev 16(5):559–589

Diel IJ, Solomayer EF, Seibel MJ et al (1999) Serum bone sialoprotein in patients with primary breast cancer is a prognostic marker for subsequent bone metastasis. Clin Cancer Res 5(12):3914–3919

Fox T, Kollman PA (1998) Application of the RESP methodology in the parametrization of organic solvents. J Phys Chem B 102(41):8070–8079

Han C, Fang S, Cao H, Lu Y, Ma Y, Wei D, Xie X, Liu X, Fei D, Zhao C (2013) Molecular interaction of PCB153 to human serum albumin: insights from spectroscopic and molecular modeling studies. J Hazard Mater 248:313–321

Hanson RN, Hua E, Adam Hendricks J, Labaree D, Hochberg RB (2012) Synthesis and evaluation of 11β-(4-substituted phenyl) estradiol analogs: transition from estrogen receptor agonists to antagonists. Biorg Med Chem 20(12):3768–3780

Heery DM, Kalkhoven E, Hoare S, Parker MG (1997) A signature motif in transcriptional co-activators mediates binding to nuclear receptors. Nature 387(6634):733–736

Henley DV, Korach KS (2006) Endocrine-disrupting chemicals use distinct mechanisms of action to modulate endocrine system function. Endocrinology 147(6):s25–s32

Hou T, Wang J, Li Y, Wang W (2011a) Assessing the performance of the MM/PBSA and MM/GBSA methods. 1. The accuracy of binding free energy calculations based on molecular dynamics simulations. J Chem Inf Model 51(1):69–82

Hou T, Wang J, Li Y, Wang W (2011b) Assessing the performance of the molecular mechanics/Poisson Boltzmann surface area and molecular mechanics/generalized Born surface area methods. II. The accuracy of ranking poses generated from docking. J Comput Chem 32(5):866–877

Jakobsson K, Thuresson K, Rylander L, Sjödin A, Hagmar L, Bergman Å (2002) Exposure to polybrominated diphenyl ethers and tetrabromobisphenol A among computer technicians. Chemosphere 46(5):709–716

Jeyakumar M, Carlson KE, Gunther JR, Katzenellenbogen JA (2011) Exploration of dimensions of estrogen potency parsing ligand binding and coactivator binding affinities. J Biol Chem 286(15):12971–12982

Jorgensen WL, Chandrasekhar J, Madura JD, Impey RW, Klein ML (1983) Comparison of simple potential functions for simulating liquid water. J Chem Phys 79(2):926–935

Kitamura S, Suzuki T, Sanoh S et al (2005) Comparative study of the endocrine-disrupting activity of bisphenol A and 19 related compounds. Toxicol Sci 84(2):249–259

Kruse AC, Hu J, Pan AC, Arlow DH, Rosenbaum DM, Rosemond E, Green HF, Liu T, Chae PS, Dror RO, Shaw DE, Weis WI, Wess J, Kobilka BK (2012) Structure and dynamics of the M3 muscarinic acetylcholine receptor. Nature 482(7386):552–556

Li Y, Burns KA, Arao Y, Luh CJ, Korach KS (2012) Differential estrogenic actions of endocrine-disrupting chemicals bisphenol A, bisphenol AF, and zearalenone through estrogen receptor α and β in vitro. Environ Health Perspect 120(7):1029–1035

Li Y, Luh CJ, Burns KA et al (2013) Endocrine-disrupting chemicals (EDCs). In vitro mechanism of estrogenic activation and differential effects on ER target genes. Environ Health Perspect 121(4):459–466

Liu H, An X, Li S, Wang Y, Li J, Liu H (2015) Interaction mechanism exploration of R-bicalutamide/S-1 with WT/W741L AR using molecular dynamics simulations. Mol Biosyst 11(12):3347–3354

Liu J, Li J, Wu Y, Zhao Y, Luo F, Li S, Yang L, Moez EK, Dinu I, Martin JW (2017) Bisphenol A metabolites and bisphenol S in paired maternal and cord serum. Environ Sci Technol 51(4):2456–2463

Maier JA, Martinez C, Kasavajhala K, Wickstrom L, Hauser KE, Simmerling C (2015) ff14SB: improving the accuracy of protein side chain and backbone parameters from ff99SB. J Chem Theory Comput 11(8):3696–3713

Margeat E, Poujol N, Boulahtouf A et al (2001) The human estrogen receptor α dimer binds a single SRC-1 coactivator molecule with an affinity dictated by agonist structure. J Mol Biol 306(3):433–442

Metskas LA, Rhoades E (2015) Conformation and dynamics of the troponin I C-terminal domain: combining single-molecule and computational approaches for a disordered protein region. J Am Chem Soc 137(37):11962–11969

Miller BR III, McGee TD Jr, Swails JM, Homeyer N, Gohlke H, Roitberg AE (2012) MMPBSA. py: an efficient program for end-state free energy calculations. J Chem Theory Comput 8(9):3314–3321

Molina-Molina JM, Amaya E, Grimaldi M et al (2013) In vitro study on the agonistic and antagonistic activities of bisphenol-S and other bisphenol-A congeners and derivatives via nuclear receptors. Toxicol Appl Pharmacol 272(1):127–136

Mongan J, Simmerling C, McCammon JA, Case DA, Onufriev A (2007) Generalized Born model with a simple, robust molecular volume correction. J Chem Theory Comput 3(1):156–169

Ng HW, Shu M, Luo H et al (2015) Estrogenic activity data extraction and in silico prediction show the endocrine disruption potential of bisphenol a replacement compounds. Chem Res Toxicol 28(9):1784–1795

Onufriev A, Bashford D, Case DA (2004) Exploring protein native states and large-scale conformational changes with a modified generalized born model. Proteins Struct Funct Bioinf 55(2):383–394

Osborne CK, Clemmons DR, Arteaga CL (1990) Regulation of breast cancer growth by insulin-like growth factors. J Steroid Biochem Mol Biol 37(6):805–809

Pike AC, Brzozowski AM, Walton J et al (2001) Structural insights into the mode of action of a pure antiestrogen. Structure 9(2):145–153

Ren XM, Zhang YF, Guo LH, Qin ZF, Lv QY, Zhang LY (2015) Structure–activity relations in binding of perfluoroalkyl compounds to human thyroid hormone T3 receptor. Arch Toxicol 89(2):233–242

Riu A, Grimaldi M, le Maire A et al (2011) Peroxisome proliferator-activated receptor γ is a target for halogenated analogs of bisphenol A. Environ Health Perspect 119(9):1227–1232

Robinson DR, Wu YM, Vats P et al (2013) Activating ESR1 mutations in hormone-resistant metastatic breast cancer. Nat Genet 45(12):1446–1451

Roe DR, Cheatham TE III (2013) PTRAJ and CPPTRAJ: software for processing and analysis of molecular dynamics trajectory data. J Chem Theory Comput 9(7):3084–3095

Rosenmai AK, Dybdahl M, Pedersen M et al (2014) Are structural analogues to bisphenol A safe alternatives? Toxicol Sci 139(1):35–47

Ruan T, Liang D, Song S, Song M, Wang H, Jiang G (2015) Evaluation of the in vitro estrogenicity of emerging bisphenol analogs and their respective estrogenic contributions in municipal sewage sludge in China. Chemosphere 124:150–155

Ryckaert JP, Ciccotti G, Berendsen HJ (1977) Numerical integration of the cartesian equations of motion of a system with constraints: molecular dynamics of n-alkanes. J Comput Phys 23(3):327–341

Salomon-Ferrer R, Götz AW, Poole D, Le GS, Walker RC (2013) Routine microsecond molecular dynamics simulations with AMBER on GPUs. 2. Explicit solvent particle mesh Ewald. J Chem Theory Comput 9(9):3878–3888

Sheng N, Li J, Liu H, Zhang A, Dai J (2016) Interaction of perfluoroalkyl acids with human liver fatty acid-binding protein. Arch Toxicol 90(1):217–227

Shiau AK, Barstad D, Loria PM et al (1998) The structural basis of estrogen receptor/coactivator recognition and the antagonism of this interaction by tamoxifen. Cell 95(7):927–937

Sindhikara DJ, Kim S, Voter AF, Roitberg AE (2009) Bad seeds sprout perilous dynamics: stochastic thermostat induced trajectory synchronization in biomolecules. J Chem Theory Comput 5(6):1624–1631

Singh T, Adekoya OA, Jayaram B (2015) Understanding the binding of inhibitors of matrix metalloproteinases by molecular docking, quantum mechanical calculations, molecular dynamics simulations, and a MMGBSA/MMBappl study. Mol BioSyst 11(4):1041–1051

Song M, Xu Y, Jiang Q et al (2006) Measurement of estrogenic activity in sediments from Haihe and Dagu River, China. Environ Int 32(5):676–681

Song M, Liang D, Liang Y et al (2014) Assessing developmental toxicity and estrogenic activity of halogenated bisphenol A on zebrafish (Danio rerio). Chemosphere 112:275–281

Teng C, Goodwin B, Shockley K et al (2013) Bisphenol A affects androgen receptor function via multiple mechanisms. Chem Biol Interact 203(3):556–564

van der Burg B, Rutteman GR, Blankenstein MA, de Laat SW, van Zoelen EJ (1988) Mitogenic stimulation of human breast cancer cells in a growth factor-defined medium: synergistic action of insulin and estrogen. J Cell Physiol 134(1):101–108

Vandenberg LN, Maffini MV, Wadia PR, Sonnenschein C, Rubin BS, Soto AM (2007) Exposure to environmentally relevant doses of the xenoestrogen bisphenol-A alters development of the fetal mouse mammary gland. Endocrinology 148(1):116–127

Vom Saal FS, Akingbemi BT, Belcher SM et al (2007) Chapel Hill bisphenol A expert panel consensus statement: integration of mechanisms, effects in animals and potential to impact human health at current levels of exposure. Reprod Toxicol 24(2):131–138

Wang J, Wolf RM, Caldwell JW, Kollman PA, Case DA (2004) Development and testing of a general amber force field. J Comput Chem 25(9):1157–1174

Wang Z, Sun H, Yao X et al (2016) Comprehensive evaluation of ten docking programs on a diverse set of protein–ligand complexes: the prediction accuracy of sampling power and scoring power. Phys Chem Chem Phys 18(18):12964–12975

Weiser J, Shenkin PS, Still WC (1999) Approximate atomic surfaces from linear combinations of pairwise overlaps (LCPO). J Comput Chem 20(2):217–230

Yang CZ, Yaniger SI, Jordan VC, Klein DJ, Bittner GD (2011) Most plastic products release estrogenic chemicals: a potential health problem that can be solved. Environ Health Perspect 119(7):989–996

Yang Y, Lv QY, Guo LH, Wan B, Ren XM, Shi YL, Cai YQ (2017) Identification of protein tyrosine phosphatase SHP-2 as a new target of perfluoroalkyl acids in HepG2 cells. Arch Toxicol 91:1697–1707

Zhao G, Perilla JR, Yufenyuy EL, Meng X, Chen B, Ning J, Ahn J, Gronenborn AM, Schulten K, Aiken C, Zhang P (2013) Mature HIV-1 capsid structure by cryo-electron microscopy and all-atom molecular dynamics. Nature 497(7451):643–646